Innovative Systems Design and Engineering
ISSN 2222-1727 (Paper) ISSN 2222-2871 (Online)
Vol 3, No.11, 2012

Simulation Model for a Frequency-Selective Land Mobile Satellite Communication Channel

Zachaeus K. Adeyemo[1], Olumide O. Ajayi[2*], Festus K. Ojo[3]

1. Department of Electronic and Electrical Engineering, Ladoke Akintola University of Technology, PMB 4000, Ogbomoso, Nigeria
2. Department of Electronic and Electrical Engineering, Ladoke Akintola University of Technology, PMB 4000, Ogbomoso, Nigeria
3. Department of Electronic and Electrical Engineering, Ladoke Akintola University of Technology, PMB 4000, Ogbomoso, Nigeria

[*]E-mail of corresponding author: skilfulltech@gmail.com

Abstract

This paper investigates a three-state simulation model for a frequency-selective land mobile satellite communication (LMSC) channel. Aside from ionospheric effects, the propagation channels for LMSC systems are also characterized by wideband effects due to multipath fading which makes the channels time-variant and exhibit frequency-selective distortion. Hence, an adequate knowledge and modelling of the propagation channel is necessary for the design and performance evaluation of the LMSC systems. A three-state simulation model for a frequency-selective LMSC channel, which is a combination of Rayleigh, Rician and Loo fading processes, is developed. The propagation characteristics of the proposed LMSC channel model are presented, and comparisons are made with the Rayleigh, Rician and Loo fading channels using bit error rate (BER) as the figure of merit. The simulation results show that the degree of fading experienced by the LMSC link depends on the length of time the mobile terminal is in a particular state or location, depending on the assumed probability of occurrence of each fading process; and it is observed from the BER results that the propagation impairment of the LMSC fading channel is relatively lower than that of Rayleigh and Loo fading channels but higher than the Rician fading channel.

Keywords: mobile, multipath fading, propagation channel, satellite communication, wideband.

1. Introduction

The use of artificial satellites for telecommunications has received increased attention for various applications such as fixed or mobile, stratospheric platforms, navigation or broadband systems [1]; and the role of satellites is changing from the traditional telephony and television (TV) broadcast services to user oriented data services [2]. The growing demand for highly-mobile multimedia access, such as Digital Video Broadcasting Satellite Services to Handheld devices (DVB-SH), at high data rates via the internet and other networks irrespective of the user's geographical location makes the role of mobile satellite communications very significant. Mobile Terminals (MTs) are designed to communicate with the satellite while in motion and can be classified as land mobile, aeronautical mobile or maritime mobile, depending on their locations on or near the earth surface [3]. The unpredictable nature, due to time-varying radio channel, however, places a limitation on the achievable data rates and quality of service (QoS) of the land mobile satellite communication (LMSC) systems. Like the terrestrial links, the LMSC links too could be frequency selective and time varying. Frequency-selective fading occurs if the maximum excess delay experienced by a signal

is greater than the symbol period. This results in rapid fluctuation in the amplitude, phase and angle of the arriving signal [4], and invariably results in signal distortion. However, the LMSC links are not exactly similar to the terrestrial cellular links because the level of propagation impairments experienced by the LMSC links depends on the geographical location, elevation angles and operating frequency band [5]. The need to investigate the characteristics of the LMSC channel is therefore very important and most of the existing works are based on single- and two-state models.

The available statistical models for LMSC channels can be categorized into two namely: single-state models and multi-state models [6]. A single-state LMSC channel model known as the Loo model is a single statistical model characterized by log-normal probability density function (pdf) and Rayleigh pdf and finds application in rural environments [7, 5]. The log-normal distribution models the shadowing attenuation affecting the line-of-sight (LOS) signal due to foliage while the Rayleigh distribution describes the diffuse multipath components. The resulting complex received signal envelope is a sum of Rayleigh and log-normal processes. Corraza-Vatalaro model is another single-state model that combines Rician and log-normal distributions used to model the effects of shadowing and LOS component [8]. The received signal envelope is assumed to be a product of Rician and log-normal processes; and the model is suitable for medium-earth orbit (MEO) and low-earth orbit (LEO) links [5]. [9] proposed an extension of Suzuki model for frequency non-selective (or flat) satellite communication channels, by considering that for most of the time a LOS component is present in the received signal. The model is a product of Rician and log-normal pdfs. The components of the Rician process are mutually correlated.

In the case of non-stationary scenarios when either the satellite or MT or both move in a large area, the propagation characteristics of such environments are appropriately characterized by the multi-state models [5]. The Lutz model is a two-state (good and bad states) statistical model based on data obtained from measurement campaigns in different parts of Europe at elevation angles between 13^{o} and 43^{o}. The good state represents LOS condition which follows Rician distribution, while the bad state follows Rayleigh distribution [10]. Higher-state LMSC channel models are based on Markov modelling approach [11, 5]. A Markov process is a stochastic process in which a system takes on discrete states. [12] proposed a three-state statistical channel model after performing L-band measurements in Japan at an elevation angle of 32^{o} [11]. The first state is LOS condition, described by Rician distribution; the second state is shadowing condition, described by log-normal distribution; and the third state is the blocked condition, described by Rayleigh distribution.

Most of the available LMSC channel models are narrowband models applicable to second-generation (2G) and third-generation (3G) systems. However, this paper focuses on the development of broadband channel models, which are more appropriate for the propagation channel characterization for future generations of LMSC systems that are expected to provide multimedia and internet services.

2. Derivation of the State Occurrence Probability Functions

Let p_A, p_B and p_C be the state occurrence probability functions for Rician, Loo and Rayleigh fading respectively. The LMSC channel condition is a function of the assumed state occurrence probabilities as shown in Figure 1. Assuming the MT is in a rich scattering environment, that is with non line-of-sight (NLOS), as in urban or suburban environments, the LMSC link experiences multipath Rayleigh fading for most of the time, p_C is assumed to be 0.4, while the remaining 60% is left between Rician and Loo distributions to share. The probability of occurrence of both Rician and Loo distributions can be given as:

$$p_A + p_B = 0.6 \tag{1}$$

The probability of occurrence for the Rician distribution, assuming the minimum elevation angle of the satellite is 10^o, is computed as [12]:

$$p_A = \frac{(90-10)^2}{q} = \frac{6400}{q} \tag{2}$$

with $q = 1.66 \times 10^4$ implies $p_A \approx 0.39$. Next, the probability of occurrence for the Loo distribution is computed by (1), which gives $p_B = 0.21$. In order to make the model flexible, p_A can be varied within the range of 0.39 and 0.21 and p_B within the range of 0.21 and 0.39. The resulting pdf of the received signal envelope is a linear combination of the Rician, Loo and Rayleigh distributions given as:

$$p(g \quad or \quad v \quad or \quad r) = p_A(g) + p_B(v) + p_C(r) \tag{3}$$

where g is the Rician distribution, r is the Rayleigh distribution and v is the distribution of the Loo model, which is the sum of log-normal and Rayleigh distributions. The Rician distribution accounts for the effect of ionospheric scintillation. The Rayleigh distribution describes the NLOS effect in the terrestrial mobile channel. The shadowing effect, which is the attenuation caused by the vegetation and foliage, is described by the Loo distribution.

3. Frequency-Selective LMSC Channel Modelling

The LMSC channel simulator presented in this paper is based on a three-state model which consists of LOS or clear (state 1), shadowing (state 2) and deep fading (state 3); and are described by Rician, Loo and Rayleigh distributions, respectively. A multi-state LMSC channel model is assumed because the relative motion and location of the transmitter and the receiver would result in varying propagation behaviour. The channel is characterized by wideband effects caused by multipath fading. The wideband effects of the LMSC channel can be well represented by the channel impulse response (CIR) '$h[n,\tau]$' of a discrete-time multipath fading channel model that can be expressed as:

$$h[n,\tau] = \sum_{l=1}^{L_p} h_l[n]\delta[n - \tau_l] \tag{4}$$ where

L_p is the number of resolvable paths; n is the discrete-time index, τ_l is the discrete relative delay of the l^{th} path; $\delta[\cdot]$ denotes Dirac delta function. The scattered waves with their respective delays are summed together to give the

impulse response of the channel. A modified Clarke-based channel model is used for the fading channel process [13].

3.1 Rayleigh Fading Process

The Rayleigh fading process r for the l^{th} path can be expressed as:

$$r_l(t) = A_l(t)e^{j\beta_l(t)} \tag{5}$$

with

$$\beta_l(t) = \omega_m \cos\alpha_l(t) + \phi_l(t) \tag{6}$$

and

$$\alpha_l = \sum_{i=1}^{N_s} \frac{2\pi i + \theta_i}{N_s} \tag{7}$$

where $\omega_m (= 2\pi f_m)$ is the maximum angular Doppler frequency shift; $A_l(t)$ is the fade amplitude (or attenuation); $\alpha_l(t)$ and $\phi_l(t)$ are the angle of arrival and phase of the l^{th} path, respectively, and are statistically independent and uniformly distributed over [-π, π); f_m is the maximum Doppler frequency shift, which is given as:

$$f_m = \frac{vf_c}{c} \tag{8}$$

where f_c is the carrier frequency, c is the speed of electromagnetic wave and v is the speed of the MT. N_s sinusoids are assumed to generate the fading process, (5) can be rewritten as:

$$r_l(t) = A_l(t)\sum_{i}^{N_s}\left(\cos\beta_{l,i}t + j\sin\beta_{l,i}t\right) \tag{9}$$

Expressing (9) in inphase and quadrature form gives:

$$r_l(t) = r_I(t) + jr_Q(t) \tag{10}$$

$r_l(t)$ is the normalized low-pass fading process whose pdf is Rayleigh. The fade envelope of $r_l(t)$ is then obtained as:

$$r_l(t) = \Re\left\{\sqrt{r_I^{\,2}(t) + r_Q^{\,2}(t)}\right\} \tag{11}$$

and the phase is:

$$\phi_l(t) = \tan^{-1}\left(\frac{r_Q(t)}{r_I(t)}\right) \tag{12}$$

where $\Re\{\cdot\}$ denotes the real part. (9) is a modified Clarke's model which is a Wide-Sense Stationary Uncorrelated Scattering (WSSUS) Rayleigh fading simulation model. The fading process is generated for all the paths and the

resultant fading process is the sum of all the L_p fading processes.

3.2 Rician Fading Process

Similarly, the normalized low-pass fading simulation model for the Rician fading can be expressed as:

$$g_l(t) = g_I(t) + jg_Q(t) \tag{13}$$

with

$$g_I(t) = \left\{r_I(t) + \sqrt{K}\cos(\omega_m t\cos\theta_0 + \phi_0)\right\} \Big/ \sqrt{1+K} \tag{14}$$

$$g_Q(t) = \left\{r_Q(t) + \sqrt{K}\sin(\omega_m t\cos\theta_0 + \phi_0)\right\} \Big/ \sqrt{1+K} \tag{15}$$

where K is the Rice factor, which represents the magnitude of the LOS signal; θ_0 and ϕ_0 are the angle of arrival and the initial phase, respectively, of the LOS component.

3.3 Loo Fading Process

The Loo simulation model is an addition of lognormal and Rayleigh processes which can be expressed as:

$$v_l(t) = \Re\left\{\left[\left(v_I(t) + r_I(t)\right) + j\left(v_Q(t) + r_Q(t)\right)\right]\exp(j2\pi f_c t)\right\} \tag{16}$$

v_I and v_Q are lognormal inphase and quadrature components, respectively. The moderate shadowing is assumed and the values of the mean (μ) and standard deviation (σ) for lognormal distribution used in the simulation are -0.115 and 0.161, respectively, given by [14].

3.4 Simulation Method

A tapped-delay line of six paths (L_p= 6), typical of wideband fading effect of mobile communications, is used to model the frequency-selective fading channels. Each tap is described by its time-varying gain a_l and the corresponding delay τ_l. The delay set for the six paths is $\tau = 0,10,20,30,40,50$ samples. The relative amplitudes (or attenuations) of the multipath components are assumed to follow the exponential power delay profile expressed as:

$$a_l = \exp(-\tau_l/30) \Big/ \sum_{i=1}^{6}\exp(-\tau_i/30), \tag{17}$$

Using the state occurrence probabilities, a set of states consisting of 1s, 2s and 3s is randomly generated and sorted in ascending order. Then for a particular run, the simulator generates the fading process corresponding to the state number as the LMSC channel, which could be Rician, Loo or Rayleigh fading channel. Separate fading signal is generated for each of the 6 paths in order to make a path independent from another. The Algorithm 1 describes the

process of generating the frequency-selective LMSC fading channel. The fading is applied to the transmitted signal through convolution.

Algorithm 1: LMSC fading channel

1. Inputs: path delays and attenuations sets
2. Outputs: fading channel
3. BEGIN
4. Get current state number
5. IF state is 1, generate Rician fading; END IF
6. IF state is 2, generate Loo fading; END IF
7. IF state is 3, generate Rayleigh fading; END IF
8. FOR k ← 1 to L_p
9. Generate the fading process corresponding to the state number
10. Apply attenuation[k] to fading signal
11. Apply delay[k] to fading signal
12. Sum fading signal for each k path

END

Simulation Parameter	**Specification**
Signaling scheme	OFDM-QPSK
Signal-to-noise ratio	0 to 18 dB
Number of paths	6
Fading spectrum	Modified Clarke's model
Number of fading sinusoids	16
Number of channel realizations	100
Path delays (samples)	[0, 10, 20, 30, 40, 50]
Average path gains (dB)	[-4.8434,-6.2911,-7.7387,-9.1864,-10.6340,-12.0817]
Rice factor (K)	3
Angle of arrival of LOS component	π/4
Angle of elevation of satellite	10^o
Mobile speeds	20 km/h, 150 km/h
Carrier frequency	2.2 GHz

4. Results and Discussion

The simulation of the fading channels was carried out in MATLAB® software environment. MATLAB codes

were written for the implementation of the models and run to generate results in form of graphs for visualization. The comparison between the LMSC fading channel and each of Rician, Loo and Rayleigh fading channels are done in terms of bit error rate (BER) performance of an OFDM-QPSK signaling scheme for signal-to-noise ratio (Eb/No) of 0 to 18 dB at mobile speed of 20 km/h and state occurrence probabilities of $p_A = 0.39$, $p_B = 0.21$ and $p_C = 0.40$ for Rician, Loo and Rayleigh fading respectively.

Table 1 shows the state occurrence probabilities for different propagation conditions. This means that at any time instant, the LMSC link can experience a transition from one state to another. The lower the probability of occurrence of any distribution, the lesser the contribution of the distribution to the resultant LMSC fading channel. The exponential power delay profile of the 6-path frequency-selective LMSC channel is shown in Figure 2. The average received power (in dB) reduces as the period of the delay (in µs) increases. This implies that the delay experienced by any specific path results in loss of the signal power. Figures 3(a) and 3(b) show the power spectral density for mobile speed of 150 km/h and 20 km/h respectively. The results show that the higher the Doppler frequency the broader the fading spectrum. That is, as the speed of the mobile terminal increases, there is a corresponding increase in the maximum Doppler frequency shift which invariably widens the fading spectrum.

Figures 4(a) and 4(b) show the frequency response of the LMSC channel for mobile speed of 150 km/h and 20 km/h respectively. The higher spikes observed for the speed of 150 km/h as compared to 20 km/h reveals that the higher the mobile speed, the higher the variation in the frequency response of the channel with time as a result of increase in the Doppler frequency shift. Figures 5 and 6 show the pdf of the Rayleigh and Rician fading process respectively. The effect of varying the Rice factor K which is the specular (or LOS) component is shown. It is observed from the graph that if K = 0, the Rician pdf reduces to the Rayleigh pdf, which implies that there is NLOS between the transmitter and the receiver.

The pdf of the Loo (Rayleigh + log-normal) fading process is shown in Figure 7. Figure 8(a) shows the pdf of the LMSC channel fading distribution, which is a combination of the Rayleigh, Rician and Loo; with the probability of occurrence of 0.39, 0.21 and 0.40 for the Rician, Loo and Rayleigh respectively. The contribution of the Rayleigh pdf to the resultant pdf of the LMSC channel is the highest, followed by the Rician pdf and the Loo pdf gives the lowest contribution. Conversely, the probability of occurrence of 0.21, 0.39 and 0.40 for the Rician, Loo and Rayleigh respectively give the LMSC channel fading distribution pdf shown in Figure 8(b). Here, the Loo pdf gives higher contribution than the Rician pdf . The reason why the Rayleigh fading contribution is made the highest is based on the assumption that the LMSC link experiences NLOS most of the time. This is true for typical urban and suburban environments.

Figures 9 and 10 show the simulated LMSC channel fading at 150 km/h and 20 km/h, respectively. The results show that the fading signal level varies more rapidly at 150 km/h but slower at 20 km/h. In Figure 11, the Rician channel gives a mean BER of 0.0609 while the LMSC channel gives a mean BER of 0.0852. The AWGN channel, the ideal channel condition needed for reliable LMSC link, gives a mean BER of 0.0228. The result from Figure 12 reveals that the Loo channel gives a mean BER of 0.1004 as against 0.0852 for the LMSC channel. Also, from Figure 13, the Rayleigh channel gives a mean BER of 0.1010 compared to 0.0852 for the LMSC channel. The comparison of all the fading channels is presented in Figure 14. The mean BER results show that the Rayleigh channel produces the worst

propagation impairments followed by the Loo channel, and then followed by the LMSC channel, while Rician channel gives the least propagation impairments.

It is observed in Figure 15 that for $p_A = 0.39$, $p_B = 0.21$ and $p_C = 0.40$, the mean BER is 0.0852; and the LMSC link is considered clear as it experiences Rician fading more of the time than the Loo fading. This is because for the Rician channel, there is a strong LOS path among the signal paths; while for the Loo channel, all the paths experience shadowing. For $p_A = 0.21$, $p_B = 0.39$ and $p_C = 0.40$, the mean BER is 0.0930 and the LMSC link is said to experience more shadowing effect than LOS. When $p_A = 0.10$, $p_B = 0.30$ and $p_C = 0.60$, the mean BER is 0.1782. This is a deep fading scenario where the LMSC link experiences multipath Rayleigh fading (with NLOS) almost the entire time share, typical of an environment with many blockages in the signal path.

5. Conclusion and Recommendations

5.1 Conclusion

The development of a simulation model for frequency-selective land mobile satellite communication channel has been analyzed, and the performance characteristics of the channel model have been evaluated in terms of bit error rate. The model assumes a three possible channel states namely clear, shadowing and deep fading. The results obtained from computer simulation show that the degree of propagation impairments of the LMSC channel depends on whether the channel is experiencing Rician fading (clear), Loo fading (shadowing) or Rayleigh fading (deep fading). The proposed simulation model is flexible because by varying the state occurrence probabilities: p_A (for Rician), p_B (for Loo) and p_C (for Rayleigh), the model is applicable to the moderate suburban, suburban and urban environments. Thus, the proposed LMSC channel model presented in this paper demonstrates the possibility of evaluating the performance of a land mobile satellite communication system based on the propagation environment under consideration.

5.2 Recommendations

For further works, the proposed model is open to modifications and empirical validations because it could be considered as a heuristic approach. This work would serve as a useful reference for researchers and engineers in the field of mobile and satellite communications.

References

[1] Castanet, L. (2000). Channel modelling and propagation impairment simulation activities within the SatNEx project, *International Journal of Satellite Communications and Networking*, vol. 29, no. 1, 2011, 1-6.

[2] Mir, R. M. (2011), Satellite Data Networks, *Technical report*. [Online] Available: http://www.cis.ohio-state.edu/~jain/cis788-97/satellite_data/ (July 6, 2011)

[3] Ilcev, S. D. (2005). *Global Mobile Satellite Communications: For Maritime, Land and Aeronautical Applications*, Netherlands: Springer Ltd. (Chapter 5).

[4] Sklar, B. (1997). Rayleigh fading channels in mobile digital communication systems, *IEEE Communications Magazine*, 90-100.

[5] Asad, M. & Abbas, M. (2011), Characterization and channel modelling for satellite communication systems, *Satellite Communications*, Blekinge Institute of Technology, Sweden, 134-151. [Online] Available:

http://www.intechopen.com/ (July 6, 2011)

[6] Abdi, A., Lau, C. W., Alouini, M. & Kave, M. (2003). A new simple model for land mobile satellite channels: first- and second-order statistics. *IEEE Trans. Wireless Comm.*, vol. 2, no. 3, 519-528.

[7] Loo, C. & Secord, N. (1991). Computer Models for Fading Channels with Applications to Digital Transmission, *IEEE Transactions on Vehicular Technology,* vol. 40, no. 4, 700–707.

[8] Corraza, G. E. & Vatalaro, F. (1994). A statistical channel model for land mobile satellite channels and its application to nongeostationary orbit systems, *IEEE Trans. Vehicular Technology,* vol. 43, no. 3, 738-742.

[9] Patzold, M., Killat, U. & Laue, F. (1998). An extended Suzuki model for land mobile satellite channels and its statistical properties, *IEEE Trans. Vehicular Technology*, vol. 47, no 2, 617-630.

[10] Lutz, E. Cygan, D. Dippold, M. Donalsky, F. & Papke, W. (1991). The land mobile satellite communication channel - recording, statistics and channel model, *IEEE Transactions on Vehicular Technology,* vol. 40, no 2, 375-386.

[11] Karaliopoulos, M. S. & Pavlidou, F. N. (1999). Modelling the land mobile satellite channel: a review," *Electronics and Communication Engineering Journal*, 235 – 248.

[12] Karasawa, Y., Kimura, K. & Minamisono, K. (1997). Analysis of availability improvement in LMSS by means of satellite diversity based on three-state propagation channel model, *IEEE Trans. Vehicular Technology,* vol. 46, no. 4, 1047-1056.

[13] Xiao, C. & Zheng, Y. R. (2003). A Statistical Simulation Model for Mobile Radio Fading Channels, *IEEE Transactions*, 144-149.

[14] Loo, C. & Secord, N. (1991), "Computer Models for Fading Channels with Applications to Digital Transmission," *IEEE Transactions on Vehicular Technology*, vol. 40, no. 4, pp. 700–707.

Dr. Z.K. Adeyemo received the B.Eng. and M.Eng. degrees in Electrical Engineering from University of Ilorin, Ilorin, Nigeria and his Ph.D. degree in Electronic and Electrical Engineering from Ladoke Akintola University of Technology (LAUTECH), Ogbomoso, Nigeria. He is a member of the IEEE and a registered member of Council for the Regulation of Engineering in Nigeria (COREN). His research interest is on signal processing in mobile communications.

Olumide O. Ajayi (M'07) became a student member of the IEEE in 2007. He received the B.Tech. degree in Electronic and Electrical Engineering from LAUTECH, Ogbomoso, Nigeria in 2008. He is a teaching assistant and currently pursuing his M.Tech. degree in the same university. His research interests include wireless communications, information security and adaptive signal processing.

Festus K. Ojo received the B.Tech. degree in Electronic and Electrical Engineering from LAUTECH, Ogbomoso, in 2008 and his M.Eng degree in Communication Engineering from Federal University of Technology (FUTA), Akure, Nigeria in 2012. His research interest is on digital communications.

Table 1. State occurrence probability of Rice, Loo and Rayleigh Distributions

Rician p_A	Loo p_B	Rayleigh p_C	LMSC channel state
0.39	0.21	0.40	clear
0.21	0.39	0.40	shadowing
0.10	0.30	0.60	deep fading

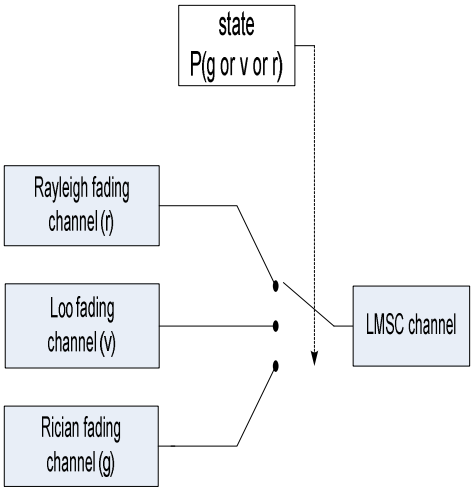

Figure 1. LMSC channel model as a function of state occurrence probability

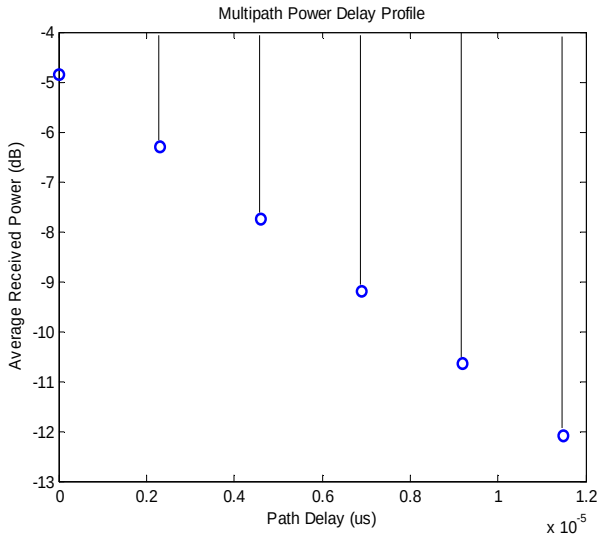

Figure 2. Power Delay Profile of the Frequency-Selective LMSC Fading

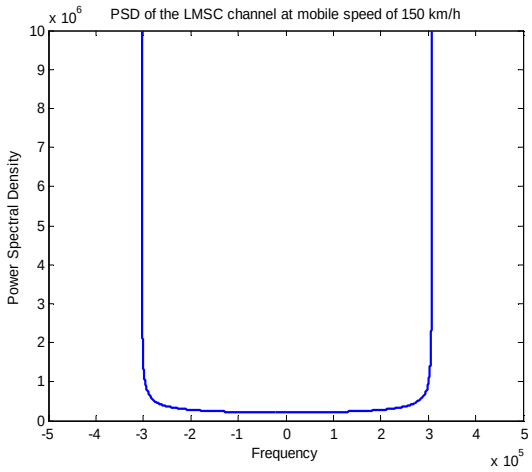

Figure 3(a). Received spectrum for the Clarke-based LMSC channel model at 150 km/h

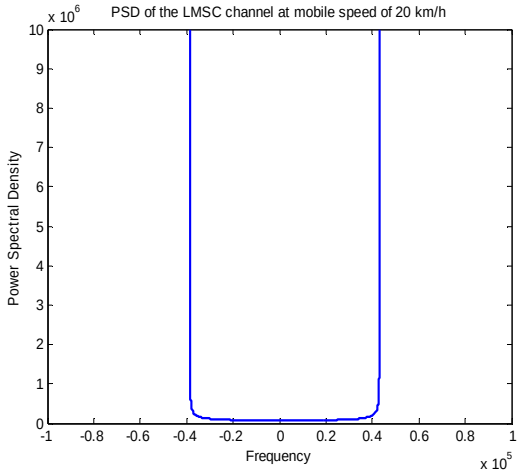

Figure 3(b). Received spectrum for the Clarke-based LMSC channel model at 20 km/h

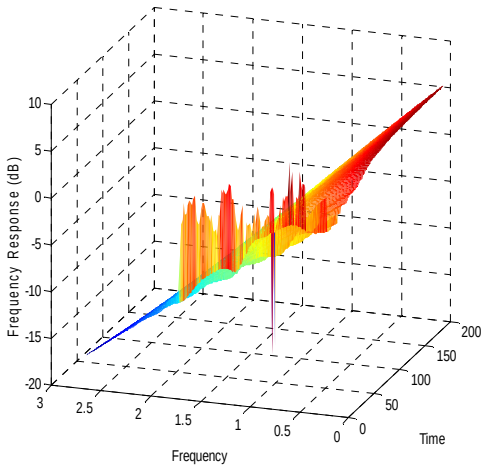

Figure 4(a). Frequency Response of the LMSC fading channel for 150 km/h

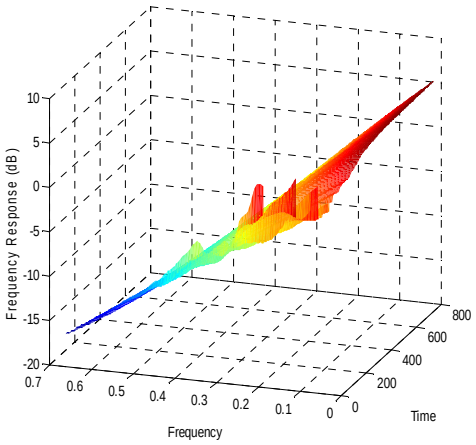

Figure 4(b). Frequency Response of the LMSC fading channel for 20 km/h

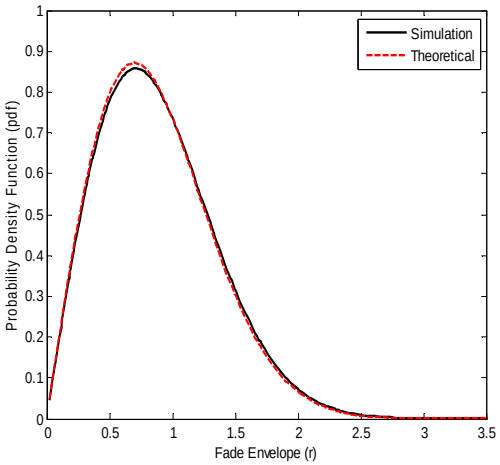

Figure 5. PDF for the Rayleigh fading distribution

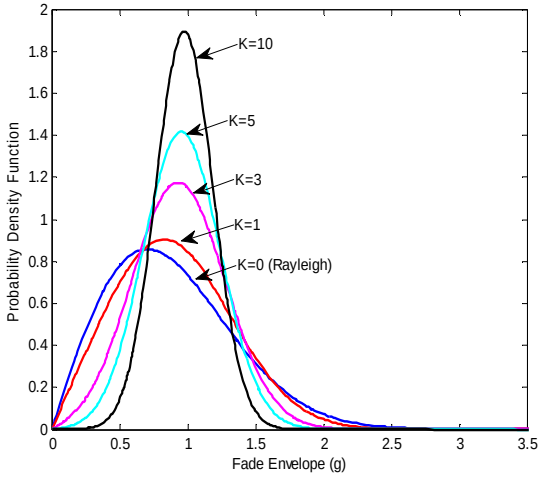

Figure 6. PDF for the Rician fading distribution

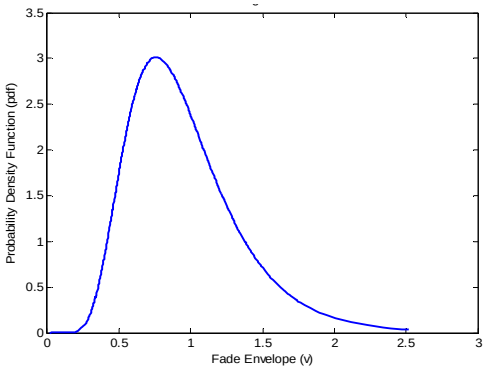

Figure 7. PDF for the Loo fading distribution

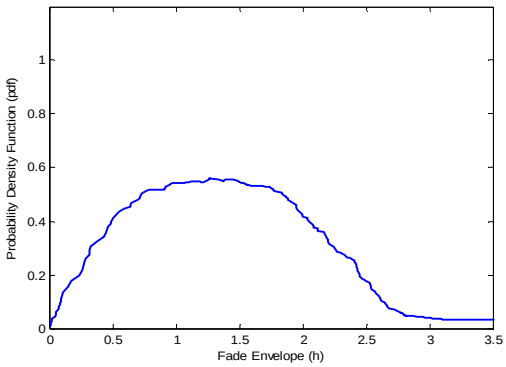

Figure 8(a). PDF for the LMSC channel fading distribution with [p_A=0.39, p_B=0.21, p_C=0.40]

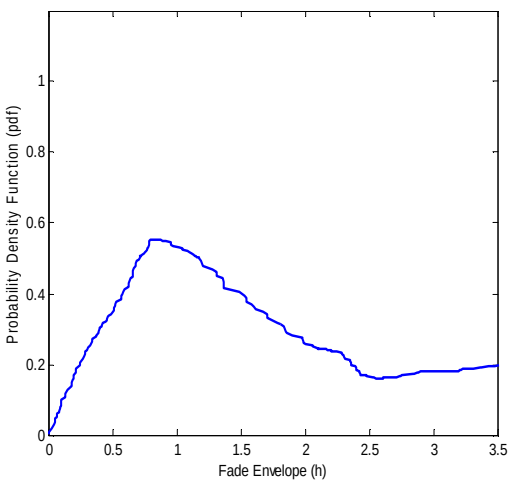

Figure 8(b). PDF for the LMSC channel fading distribution with [p_A=0.21, p_B=0.39, p_C=0.40]

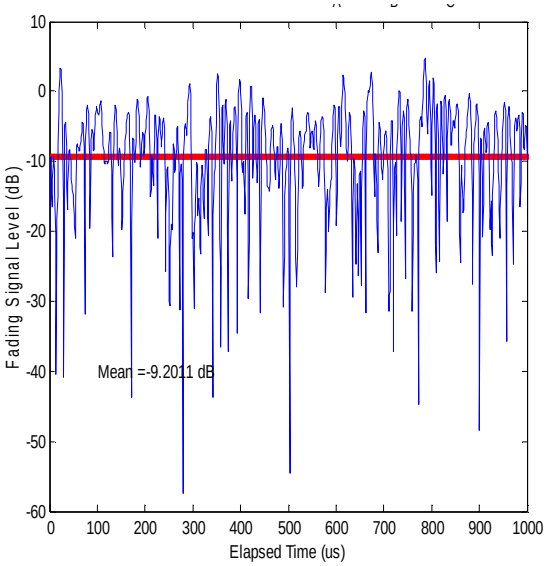

Figure 9. Simulated LMSC channel fading at 150km

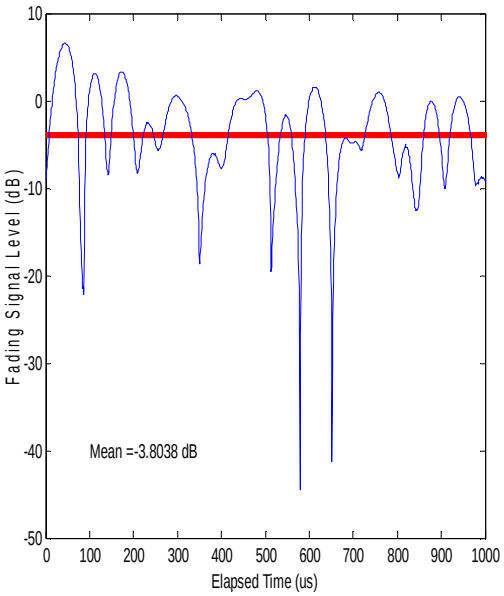

Figure 10. Simulated LMSC channel at 20 km/h

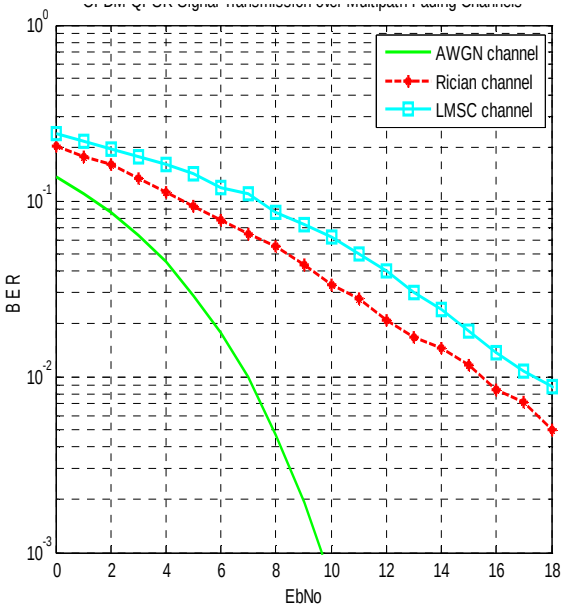

Figure 11. BER comparison of the Rician and LMSC channels at 20 km/h

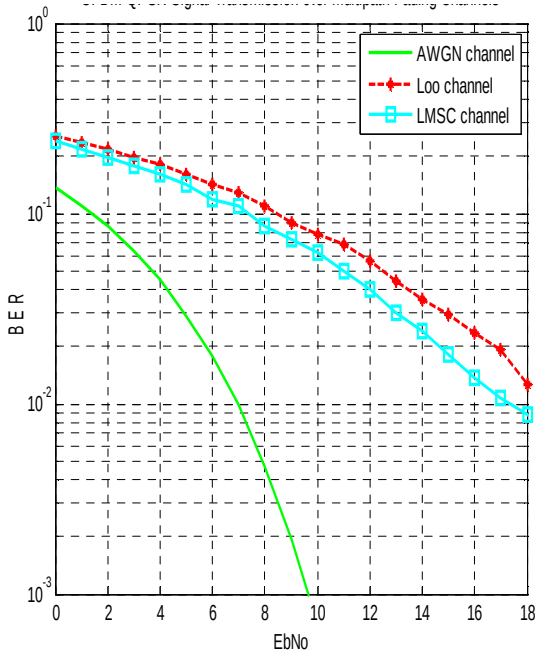

Figure 12. BER comparison of the Loo and LMSC channels at 20 km/h

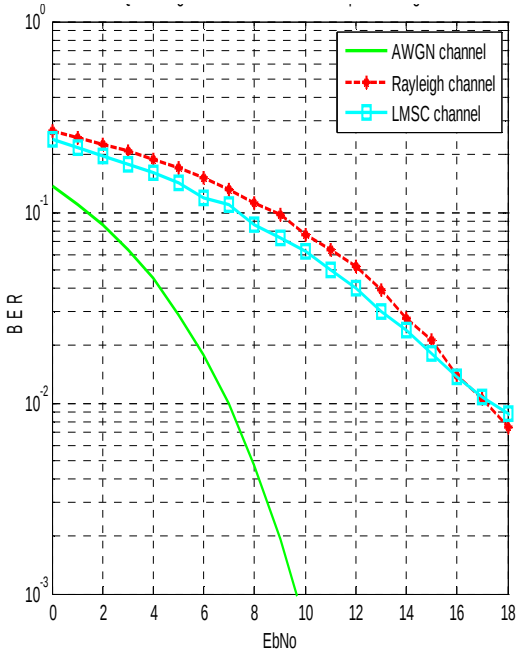

Figure 13. BER comparison of the Rayleigh and LMSC channels at 20 km/h

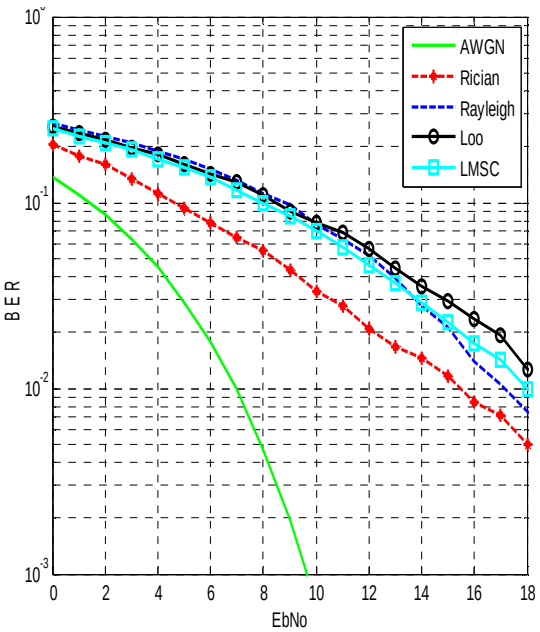

Figure 14. BER comparison of all the fading Channels at 20km/h

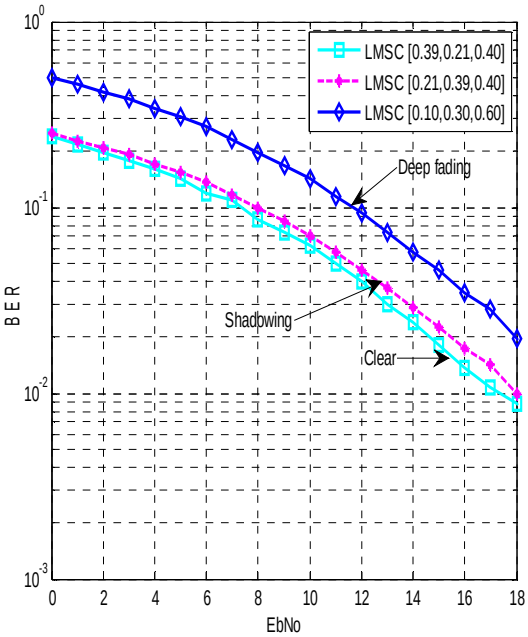

Figure 15. Effect of the state occurrence probabilities on the LMSC channel at 20km/h